Semester Thesis

Design of a Quantum Teleportation Experiment and Qubit Simulation

Florian Lüthi
Supervisor: Prof. Dr. A. Wallraff

September 6, 2012

Abstract

A quantum computer works on the basis of superposition of two-level systems (qubits). It performs certain tasks, for example factorization of numbers, much faster than a normal computer. Should it one day be possible to construct quantum computers with many qubits, a possibility to perform computations is given using only teleportation and single-qubit operations.

In this semester thesis a chip has been designed, on which the quantum teleportation experiment can be performed. Other experiments were designed to analyze the coupling between coplanar wave guide resonators and to be able to easily test different realizations of qubits.

As a last part of the thesis, different quantum bits were simulated. This is done to get an idea about the characteristic quantities of the different possible realizations of a qubit. Based on the already used qubits, it was tried to improve their properties.

Contents

1 Introduction

Quantum mechanics has become the most successful physical theory so far. There is no experiment in contradiction with it. And further on, it is very general: it describes the microscopic world in astonishing precision, but it describes as well properties of the whole universe, see eg. [1]. If we want to state something about a quantum mechanical system, we have to do this using quantum information. It does not behave like classical information. Imagine a classical system, in which there is an object in one of two possible states, eg. a ball which is on the table or on the floor. Of course, these two possibilities exclude each other. But in quantum mechanics, it can be in both states at the same time - the ball can be on the floor and on the table simultaneously. This is a superposition of states. Thus, the quantum mechanical piece of information, the quantum bit, can not just exclusively take the value 0 or 1, like the classical bit, but it can have both values at the same time, compare eg. [2].

But why should we be interested in this kind of information? Using it and computing with it enables us to perform calculations we would not be able to do with classical computers. For example, using classical computers, it takes an exponentially growing amount of computing time to factorize a number. Many codes are based on this fact: If you have to factorize a large number, you will have a huge amount of work to do. If no one is able to perform this fast enough, the code is safe. But if we use quantum information, the amount of time required to factorize a number will only grow polynomial with the number (Shor's factoring algorithm), see [4]. This would mean, that most of the classical codes are not safe anymore.

Another interesting application is Grover's search algorithm, which enables one to search a (unordered) database in $\mathcal{O}(\sqrt{n})$ steps and using only $\mathcal{O}(log(n))$ storage space [5]. The fastest classical algorithm for this task is the linear search, which needs $\mathcal{O}(n)$ steps. As well, several NP complete problems could be solved much faster.

Such a quantum bit, a qubit, can be realized in different ways. One approach is to use a macroscopic superconducting circuit on a chip to build a quantum mechanical two level system. In the special setup which is used here, this was first realized in [6]. For an implementation like this one, it is possible to borrow fabrication techniques for conventional integrated circuits.

2 Theory

2.1 The Quantum Bit

Unlike a classical bit which is represented by either 0 or 1, a quantum bit lives in a two dimensional Hilbert space. We can choose a basis of this space, for example the two orthogonal and normalized state vectors $|0\rangle$ and $|1\rangle$. We will think of $|0\rangle$ being the ground state, and $|1\rangle$ the excited state of our system. As mentioned in section 1, these two states can be superposed. The condition of normalization requires, that for any superposition state $|\psi\rangle = \alpha|0\rangle + \beta|1\rangle$ we have $|\alpha|^2 + |\beta|^2 = 1$. Since any global phase does not matter, we can just look at the relative phase between α and β, let's call it φ. We can also write $|\psi\rangle$ as

$$|\psi\rangle = \cos\left(\frac{\theta}{2}\right)|0\rangle + \mathrm{e}^{i\varphi}\cos\left(\frac{\theta}{2}\right)|1\rangle \tag{1}$$

with $0 \leq \theta < \pi$ and $0 \leq \varphi < 2\pi$. A geometrical representation of this would be the 2-sphere. The state vector $|0\rangle$ is north pole, and the $|1\rangle$ is the south pole. Any mixed state is represented by a point lying on the surface of the sphere, see Fig. 1. Like this, the normalization condition is always fulfilled.

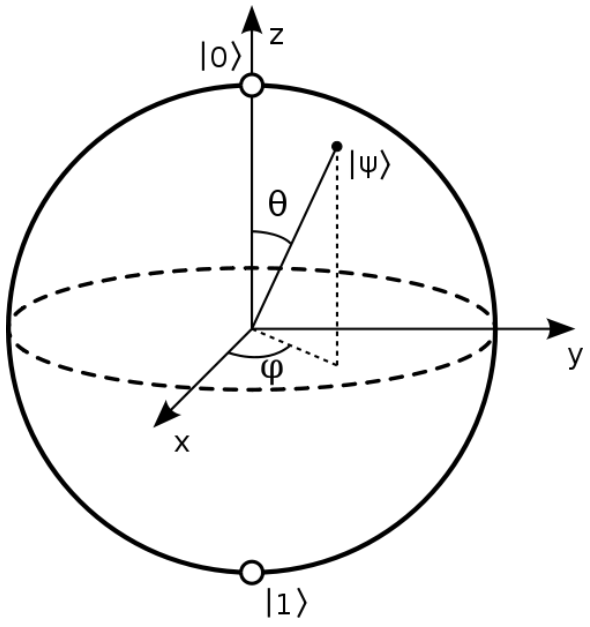

Figure 1: Geometrical representation of the Bloch sphere, ψ is a mixed state.

2.2 Entanglement

If we have more than one quantum bit, the Hilbert space of the total system is the tensor product of the individual system. If we have n qubits, the dimension of the Hilbert space is 2^n. In this space exist state vectors, which can not be described only having a product of the individual two dimensional spaces. These non-separable vectors are said to be entangled states. These entangled states will allow us to do a quantum Teleportation, cf section 2.9.

2.3 Josephson Junction

A Josephson junction is a non linear circuit element, which will be described here briefly. It consists of two superconducting electrodes, separated by a thin oxide layer, see Fig. 2. This circuit element has the advantage, that it has an anharmonic energy spectrum, enabling one to address two different states separately - this is what we need to have in order to control a two level system. Further on, a Josephson junction can be operated at arbitrarily low temperatures. We will need this, since the energy required to go from the state $|0\rangle$ to the state $|1\rangle$, namely $\hbar\omega_{01}$ has to be much larger than the thermal fluctuation with typical energies of $k_B T$. The qubits used have a transition

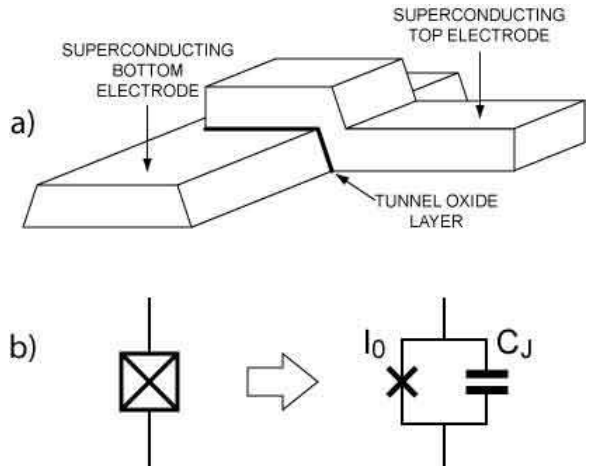

Figure 2: a) A Josephson junction made of superconducting conductors. b) Representation of a Josephson junction, the figure is taken from [3].

frequency $\omega_{01} \approx$ 3-10 GHz. This means, that the temperature T has to be in the order of 10 mK. Also, the Josephson junction works in a non-dissipative way: it has no losses in energy when transporting an electronic signal over the chip, and energy is contained in the qubit itself. The Josephson junction has two characteristic quantities, the Josephson capacity C_J and the Josephson

energy E_J which is the potential energy stored in the junction when a super current flows through it.

2.4 Cooper Pair Box

We are aiming to construct a charge qubit. A Cooper pair box is a prototype of it. It consists of a superconducting electrode, the island, which is connected to another superconducting electrode, the reservoir, via a Josephson junction with C_J and E_J. One can think of the junction allowing Cooper pairs to couple coherently between island and reservoir, with a capacitance in parallel [7]. One can apply a gate voltage V_G such that Cooper pairs are electrostatically induced to tunnel, compare Fig. 3.

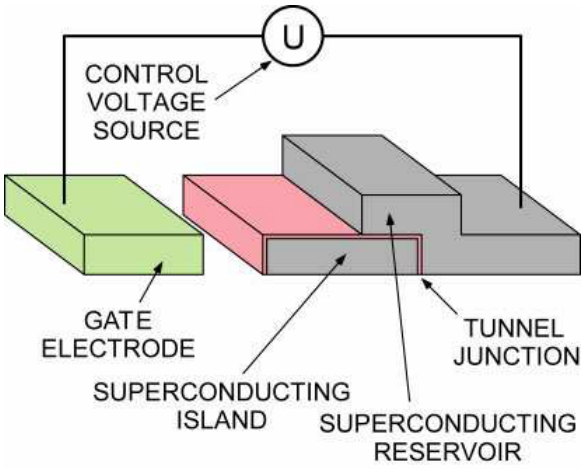

Figure 3: Schematic representation of a Cooper pair box. Island and reservoir are coupled with a Josephson junction, island and gate are coupled capacitively. Figure from [8].

There is only one degree of freedom in the Cooper pair box, and this is the number n of excess Cooper pairs on the island. A basis of the states of the Cooper pair box is given by the eigenstates $|n\rangle$ of the associated operator $\hat{n}$. The Hamiltonian of the system consists of an electrostatic part and a part describing the coherent tunneling of Cooper pairs through the junction. In [10] is shown that the Hamiltonian is

$$H_{CPB} = 4E_C(\hat{n} - n_g)^2 - E_J \cos(\hat{\varphi}) \tag{2}$$

$$= 4E_C(\hat{n} - n_g)^2 + \frac{E_J}{2} \sum_N (|n\rangle\langle n+1| + |n+1\rangle\langle n|). \tag{3}$$

In this Hamiltonian, $E_C = e^2/2C_\Sigma$ denotes the electrostatic charging energy where $C_\Sigma = C_J + Cg$ is the total capacitance of the Cooper pair box. n_g is the dimensionless gate charge given by $n_g = C_g V_g/2e$, and E_J is the Josephson energy mentioned above which is proportional to the area of the tunnel junction.

We will run the Cooper pair box in the charge regime, where $4E_C \gg E_J$. Fluctuations in the gate charge n_g will lead to fluctuations of the transition frequency ω_{01} of the qubit. At the sweet spot ($n_g = 1/2$), which is a degeneracy point, it immune against these fluctuations in first order, see Fig. 4. This allows longer coherence times.

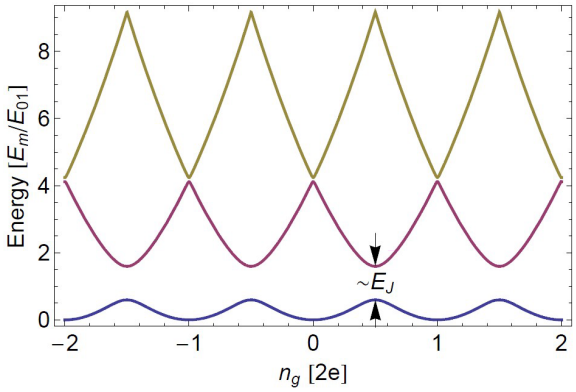

Figure 4: An energy level diagram of a Cooper pair box. The colored lines are the ground state and first and second excited state of a CPB with $E_J = E_C$. The units are given in units of the transition energy. The sweet spot is at $n_g = 1/2$. Figure from [9].

2.5 Split Cooper Pair Box

For a better control of the qubits, a split Cooper pair box is used. The difference to a normal CPB is that the junction between island and reservoir is split into two junctions. These can have different Josephson energies E_{J_1} and E_{J_2} and different superconducting phases θ_1 and θ_2 across them, compare Fig. 5. By applying a gate voltage V_g we can control n_g. If we send a magnetic flux Φ through the loop, we can change the effective Josephson energy of the split Cooper pair box and obtain, see [7],

$$E_J^{eff} = (E_{J_1} + E_{J_2}) \cos\left(\pi \frac{\Phi}{\Phi_0}\right), \tag{4}$$

where $\Phi_0 = h/2e$ denotes the flux quantum.

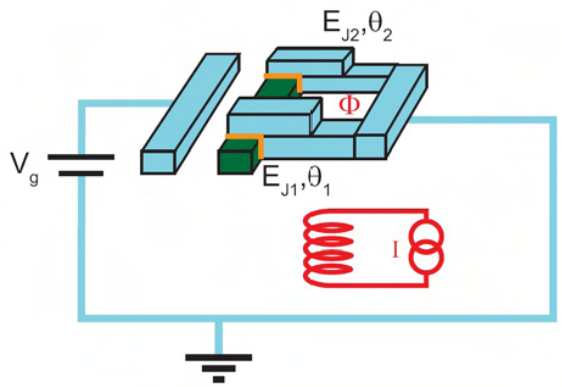

Figure 5: Schematic representation of a split CPB. Island and reservoir are connected with two junctions, each with it's own Josephson energy and phase difference. The effective E_J can be tuned by applying a magnetic flux through the split CPB. Figure from [9].

2.6 Transmon

A cooper pair box is sensitive to fluctuations in the gate charge n_g, as mentioned above. But if we increase the ratio E_J/E_C, the energy levels become extremely flat. This again makes the transmission frequency of the qubit immune to charge fluctuations. The drawback is some loss of anharmonicity. But this is not too serious, since the flattening of the bands obeys an exponential law in E_J/E_C while the loss in anharmonicity only follows a weak power law, [11], [12] (compare fig. 6). In order to decrease the charging energy E_C, we need to have a large capacitance between reservoir and island. This can be done by enlarging the areas of both parts or making fingers. Such Cooper pair boxes are called "transmons" In section 4, some simulations of transmons with different extensions will be presented. These simulations are done in order to optimize the properties of the transmon. In Fig. 7, there is a comparison between a normal CPB and the much larger transmon.

2.7 Transmission Line Resonator

A transmission line can be schematically represented as a two wire line.It can be shown ([2], [7]) that it is equivalent to a RLC oscillating circuit. A resonator can be made by opening the two ends of the transmission line (for further explanations see [7]). Here, two types of resonance can occur. The first is the so called $\lambda/2$ resonance. It occurs, when the length l of the resonator is an integer multiple of half the wavelength λ of the wave ($l = n \cdot \lambda/2, n \in \mathbb{N}$). This kind of resonance has a high impedance, and we

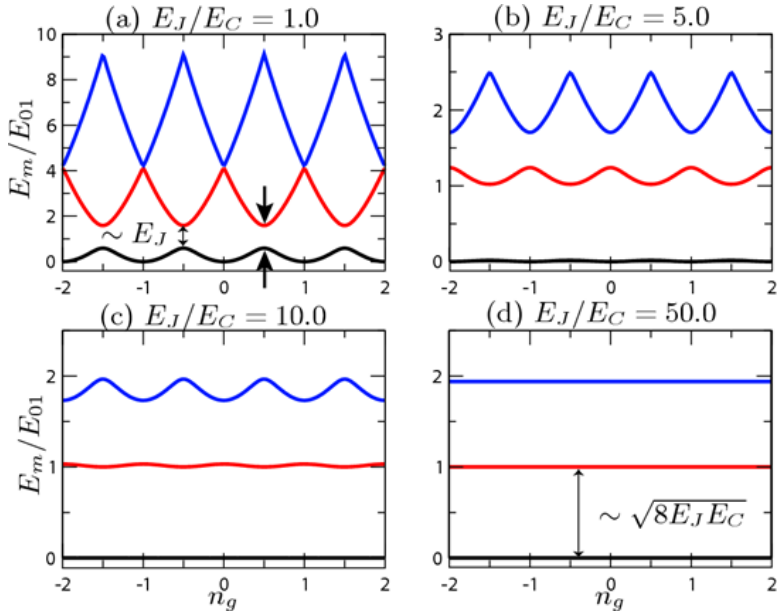

Figure 6: Energy levels of a transmon (energy eigenvalues of the Hamiltonian (3)), with different E_J/E_C ratios. As in Fig. 4, the energy axis is given in units of the transition energy E_{01} at the sweet spot ($n_g = 1/2$). Figure from [11].

will use it in our circuit. The other kind of resonance occurs when the length of the transmission line is an odd multiple of a quarter of the wavelength ($l = (2n+1) \cdot \lambda/4$). In this case, we have a high admittance resonance. The resonance frequency for the (here used) $\lambda/2$ resonators is

$$\omega_{0,n} = \frac{n\pi}{l\sqrt{L_l C_l}}, \tag{5}$$

where L_l and C_l are the inductance, respectively capacitance per unit length of the two wires.

Capacitive Coupling is needed to drive the resonator.This is because it can not be directly connected to another transmission line from the "outside world", this would destroy the quality factor Q of the resonator, and the radiation would escape quickly. Therefore, we connect the resonator via capacitors with small capacitance to the in- and output transmission lines. This causes a large impedance mismatch. This causes the photons to be reflected there like at a mirror, only a small amount of them will pass. The coupling will shift the resonance frequency by adding an effective capacitance, and it will influence the Q.

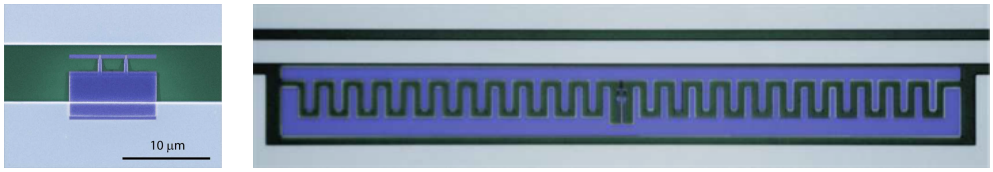

(a) Split CPB (b) Transmon, the length of the structure is 300 μm

Figure 7: Comparison between a split CPB and a transmon. Consider the different length scales, from [7]

A Coplanar Wave Guide Resonator (CPW) is one possible realization of a transmission line on a chip. It is the two dimensional version of the coaxial cable. It has the ground in the same plane like the center pin, compare Fig. 8. The characteristic impedance is determined by the ratio a/b, the substrate hight h and the dielectric constant of the substrate.

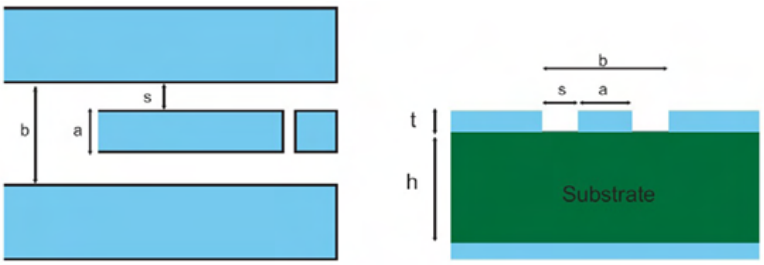

Figure 8: A conductor backed coplanar waveguide. The geometry determines the impedance. Figure from [9].

2.8 Circuit Quantum Electrodynamics

Cavity Quantum Electrodynamics (CQED) describes the interaction between atoms and photons with discrete modes in a cavity. A simple version of this system is a two-level atom which couples to a cavity. The cavity is described by a harmonic oscillator whose excitations are photons. This system is described by the Jaynes-Cummings Hamiltonian H_{JC}, see [13].

$$H_{JC} = \hbar\omega_r(a^\dagger a + 1/2) + \hbar\frac{\omega_a}{2}\sigma_z + \hbar g(a^\dagger\sigma^- + a\sigma^+) + H_\kappa + H_\gamma \qquad (6)$$

In this equation, the first term represents the electromagnetic field. Each photon has there an energy $\hbar\omega_r$. The second term represents the atom to be a spin-1/2 particle, which has a transition energy of $\hbar\omega_a$. The third term is due to the dipole interaction: an atom can emit $(a^\dagger\sigma^-)$ or absorb $(a\sigma^+)$ a

photon to/from the field, with rate g. So, the coherent dynamics is described with these three terms. The fourth term is the coupling of the cavity to the continuum. This produces a cavity decay rate $\kappa = \omega_r/Q$. The fifth term describes the spontaneous decay of the excited state of the qubit, a photon gets emitted into the environment. This is visualized in Fig. 9.

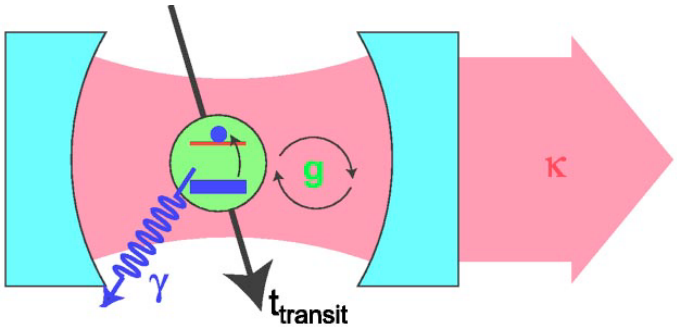

Figure 9: Representation of a cavity QED system. An atom (two-level system) which has a spontaneous decay rate γ passes a cavity with decay rate κ. During the time $T_{transit}$ it is in the cavity, it interacts coherently with a single mode of the electromagnetic field, which is trapped in between the mirrors, with coupling strength g. Figure from [13].

If we have zero detuning $\Delta = \omega_r - \omega_a = 0$ between atom and cavity, the eigenstates of the Hamiltonian H_{JC} (without damping), see eq. 6, are the maximally entangled atom-field states $|\overline{\pm,0}\rangle = (|\uparrow,1\rangle \pm |\downarrow,0\rangle)/\sqrt{2}$, [7]. Starting with an initial state $|\downarrow,0\rangle$ with an excited atom an no photons, it will change to a photon and back again. This happens at the vacuum Rabi frequency g/π. We can look at the excitation being half the time a photon and half the time an excited state of the atom, the decay rate of $|\overline{\pm,0}\rangle$ is given by $(\kappa+\gamma)/2$. When it takes a long time for the atom to decay or the photon to be lost, i.e. when many oscillations can be completed, the system is in the strong coupling limit of cavity QED ($g > \kappa, \gamma, 1/T_{transit}$) [13], [7].

CQED With Superconducting Circuits Not only optical system can be used as cavity QED systems, but for instance also circuits. In this case, the cavity is a one-dimensional transmission line resonator (compare section 2.7) and the artificial atom is a Cooper pair box (compare section 2.4). The Cooper pair box then couples capacitively to the electromagnetic field of the resonator. This situation is schematically represented in Fig. 10.

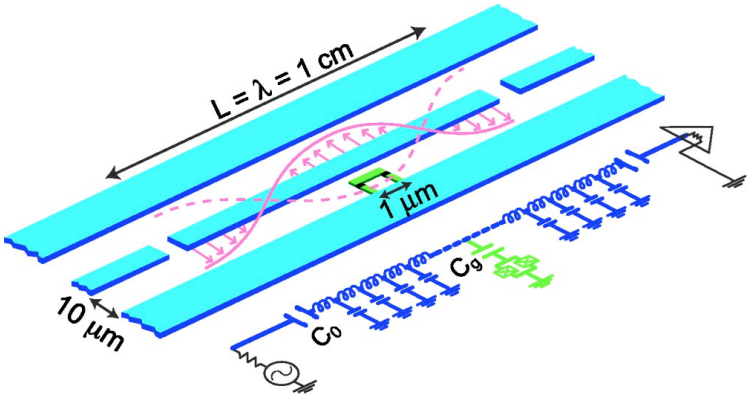

Figure 10: Schematic representation of a qubit in a superconducting circuit. A cooper pair box, acting as qubit, is placed between the lines of a superconducting coplanar wave guide resonator. The CPB is capacitively coupled to the center trace at the maximum voltage of the first harmonic of the standing wave. This yields a strong electric dipole interaction between qubit and individual photons of the resonator. The indicated lengths have to be considered as an order of magnitude. Figure from [13].

2.9 Teleportation of a Quantum State

The first experiment designed, cf section 3.2, aims to implement a quantum teleportation. Here, we will briefly discuss the basic idea of the quantum teleportation.

Due to the No-Cloning-Theorem [14], it is not possible to copy a quantum state: If we have a particle A in the state $|\varphi\rangle$ we can not bring a particle B in the same state $|\varphi\rangle$ as particle A without changing the state of the particle A. But it is not forbidden to bring particle B into the state $|\varphi\rangle$ and at the same time changing the state of particle A. This would be a teleportation of quantum information, a quantum teleportation. Note, that this differs from swapping the states of the qubits. In the swap operation, the states of two qubits are swapped, but for this, a quantum channel is needed. For quantum teleportation, we only need to transmit classical information and thus a classical channel is enough (provided that we have a third particle we can use).

The naive ansatz is to measure the state $|\varphi\rangle$ of particle A and bring B into this state. This does of course not work, since $|\varphi\rangle$ could be in a superposition state, and if we measure $|\varphi\rangle$ we will just measure an eigenstate of the operator. This is not the whole information, and thus we are not able to extract the whole quantum information out of $|\varphi\rangle$ like this.

We need to have two two-level systems A and B which are maximally entangled to each other. Alice has one of these, A, and Bob has the other, B. Then, Alice wants to transmit the state $|\varphi\rangle_C = \alpha|0\rangle_C + \beta|1\rangle_C$ of a two-level system C to Bob (only Alice has access to C, Bob has not), such that after the transmission the state of B, $|\varphi\rangle_B$ is the same as the state of C before: $|\varphi\rangle_B = \alpha|0\rangle_B + \beta|1\rangle_B$.

Let now the two-level systems A and B be in a maximally entangled state, for example in the first of the four Bell states

$$
\begin{aligned}
|\Phi^+\rangle_{AB} &= \frac{1}{\sqrt{2}}\left(|0\rangle_A \otimes |0\rangle_B + |1\rangle_A \otimes |1\rangle_B\right), \qquad (7)\\
|\Phi^-\rangle_{AB} &= \frac{1}{\sqrt{2}}\left(|0\rangle_A \otimes |0\rangle_B - |1\rangle_A \otimes |1\rangle_B\right),\\
|\Psi^+\rangle_{AB} &= \frac{1}{\sqrt{2}}\left(|0\rangle_A \otimes |1\rangle_B + |1\rangle_A \otimes |0\rangle_B\right),\\
|\Psi^-\rangle_{AB} &= \frac{1}{\sqrt{2}}\left(|0\rangle_A \otimes |1\rangle_B - |1\rangle_A \otimes |0\rangle_B\right),
\end{aligned}
$$

where A belongs to Alice and B to Bob. So Alice has now two particles, A and C. The total system writes now as

$$
|\Phi^+\rangle_{AB} \otimes |\Psi\rangle_C = \frac{1}{\sqrt{2}}\left(|0\rangle_A \otimes |0\rangle_B + |1\rangle_A \otimes |1\rangle_B\right) \otimes \left(\alpha|0\rangle_C + \beta|1\rangle_C\right), \qquad (8)
$$

where $|\Psi\rangle_C = \alpha|0\rangle_C + \beta|1\rangle_C$ is the initial state of particle C. Using that

$$
\begin{aligned}
|0\rangle \otimes |0\rangle &= \frac{1}{\sqrt{2}}\left(|\Phi^+\rangle + |\Phi^-\rangle\right), \qquad (9)\\
|0\rangle \otimes |1\rangle &= \frac{1}{\sqrt{2}}\left(|\Psi^+\rangle + |\Psi^-\rangle\right),\\
|1\rangle \otimes |0\rangle &= \frac{1}{\sqrt{2}}\left(|\Psi^+\rangle - |\Psi^-\rangle\right),\\
|1\rangle \otimes |1\rangle &= \frac{1}{\sqrt{2}}\left(|\Phi^+\rangle - |\Phi^-\rangle\right),
\end{aligned}
$$

we can write the state of the total system (8) as

$$
\begin{aligned}
|\Phi^+\rangle_{AB} \otimes |\Psi\rangle_C = \frac{1}{2}\big(&|\Phi^+\rangle_{AC} \otimes (\alpha|0\rangle_B + \beta|1\rangle_B) + |\Phi^-\rangle_{AC} \otimes (\alpha|0\rangle_B - \beta|1\rangle_B) \qquad (10)\\
&+ |\Psi^+\rangle_{AC} \otimes (\beta|0\rangle_B + \alpha|1\rangle_B) + |\Psi^-\rangle_{AC} \otimes (\beta|0\rangle_B - \alpha|1\rangle_B)\big),
\end{aligned}
$$

which is just a basis change on Alice's part of the system. Note that so far no operation has been performed. The actual teleportation process starts when

Alice measures her two qubits in the Bell-basis (she projects (10) on to the Bell-basis with the projection operators $|\Phi^+\rangle\langle\Phi^+|$ and analog for the other states).The state (10) collapses under this measurement. This gives her one of the following states (each with equal probability):

- $|\Phi^+\rangle_{AC} \otimes (\alpha|0\rangle_B + \beta|1\rangle_B)$
- $|\Phi^-\rangle_{AC} \otimes (\alpha|0\rangle_B - \beta|1\rangle_B)$
- $|\Psi^+\rangle_{AC} \otimes (\beta|0\rangle_B + \alpha|1\rangle_B)$
- $|\Psi^-\rangle_{AC} \otimes (\beta|0\rangle_B + \alpha|1\rangle_B)$

This now means that Alice's two particles are now entangled to each other (and are again in a Bell state), and the entanglement between A and B is broken. In each possible outcome of the measurement, particle B is in a state that resembles the original state $|\varphi\rangle_C$. Now we have to apply a unitary operation on B such that B is in the desired state afterwards. Since Alice has measured (10) in the Bell Basis, she knows in which of the four possible states the particle B is in. Therefore, Alice has to transmit Bob in a classical way this information (two Bits). Now Bob knows which operation he has to perform, such that his particle has afterwards the desired state $\alpha|0\rangle_B+\beta|0\rangle_B$:

- If Alice's result is $|\Phi^+\rangle_{AC}$, Bob already has the correct state, and he does nothing.
- If Alice's result is $|\Phi^-\rangle_{AC}$, Bob applies the third Pauli Matrix σ_3 on his particle, and he gets the desired state as well.
- If Alice's result is $|\Psi^+\rangle_{AC}$, Bob applies the first Pauli Matrix σ_1 on his particle, and he is done again.
- If Alice's result is $|\Psi^-\rangle_{AC}$, Bob applies i times the second Pauli Matrix on his particle, $i\sigma_2$, and he obtains the final result.

The scheme of this is shown in Fig. 11.

Note, that after the teleportation the states of the particles A and C are just eigenstates of the measured operator. This means, that we do not have a contradiction to the No-Cloning-Theorem. Also, no energy or mass has been transported, and therefore teleportation is consistent with energy-conservation. For each state one wants to teleport, Alice and Bob need an entangled pair of particles. And for each teleportation, Alice needs to transmit information over a classical channel. This can be intercepted, but the information one gets from this does not help anything: the interceptor

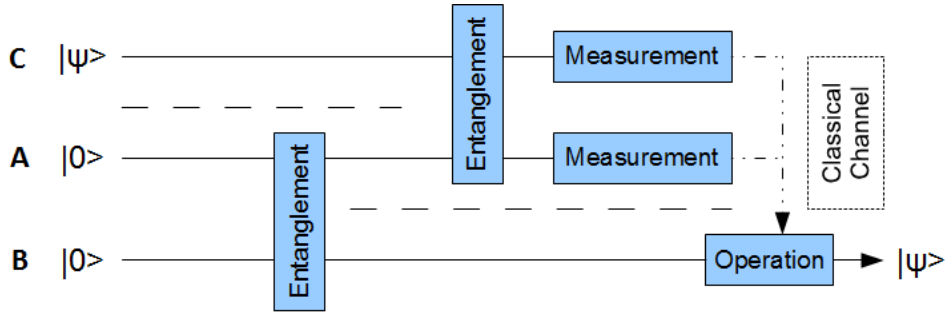

Figure 11: The scheme of a quantum teleportation. The state $|\Psi>$ is teleported from the first to the third qubit.

only knows which gate Bob has to apply, but he does not have the particle and thus can not reproduce the desired state.

Of course, the two-level systems A, B and C also can be qubits. The experiment will be implemented using qubits as two-level systems. Quantum teleportation was first realized by Zeilinger et al. in 1997 with photons [15].

3 Designed Chips

In this section, the designed chips are presented, and also why they are designed like this is presented. But first of all, it is described how designing is done and what the different elements on a chip are.

3.1 Basics

The chip design is done in Mathematica. There, a two dimensional drawing is made on which the elements of the chip are placed (in fact the graphic is on a plane in three dimensional space, allowing us to mirror it). These elements were already implemented as functions in a library, and they could just be placed on the correct spot and with the correct orientation. This placing is done by giving the functions as argument the coordinates.

The chip can be controlled via 8 pins on each side. One can send signals for example signals into a resonator or a current through a flux line via these pins.

There are many different objects which need to be placed on a chip, compare Fig. 12. In the following, the different elements will be explained in a bit more detail.

In Fig. 13 we can see two cut-outs of Fig. 12. The white parts will become covered with a superconducting metal layer which is superconducting at low

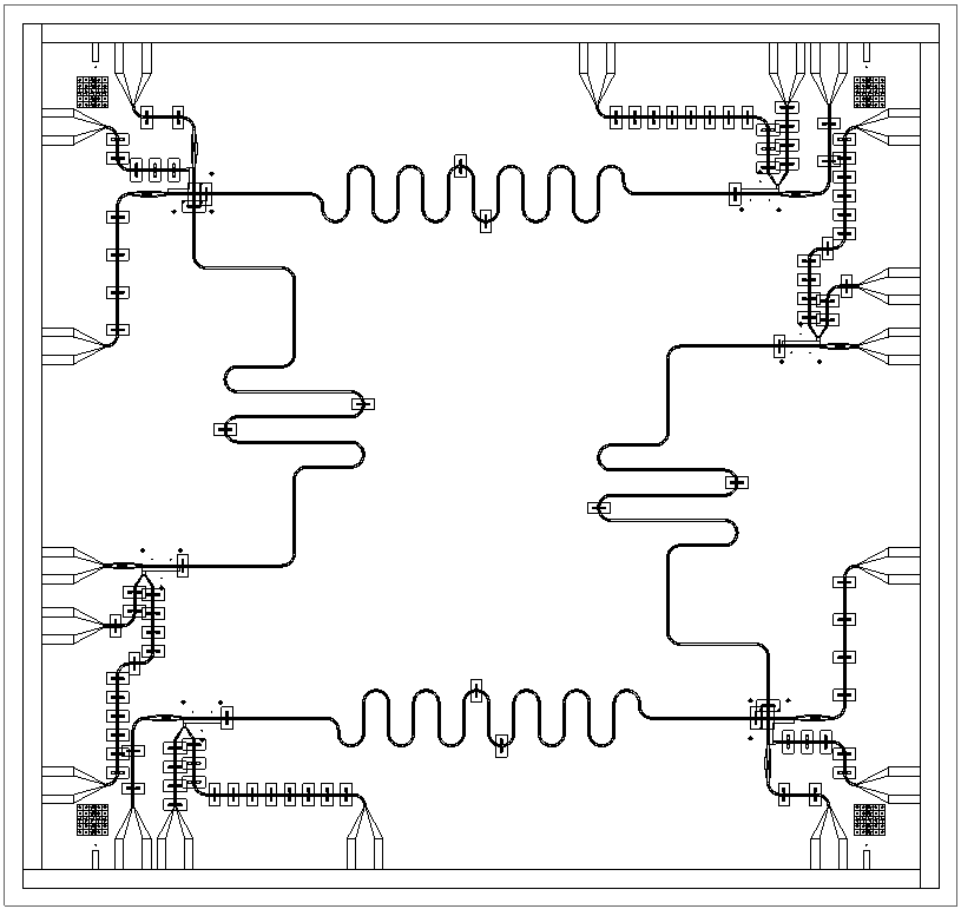

Figure 12: The chip design of a quantum teleportation experiment. There are two identical experiments on the same chip, such that the effort of measuring one experiment is smaller.

enough temperatures. This will then be the ground of the chip. The parts which are colored are not covered by a metal layer, and thus be insulating. Fig. 12 shows the most important structures (colored) used on the chip:

- The light green and big structures in Fig. 13a are the gateways which connect the pins with the flux lines and resonators. Via these pins, currents can be controlled and sent on the chip.
- The red structures in Fig. 13a and 13b are the couplers. They capacitively couple the control-current applied at the pins to the states in the resonator. For the resonator, they act like mirrors in an optical cavity: the wave is reflected at them. The finger-like structures (partially

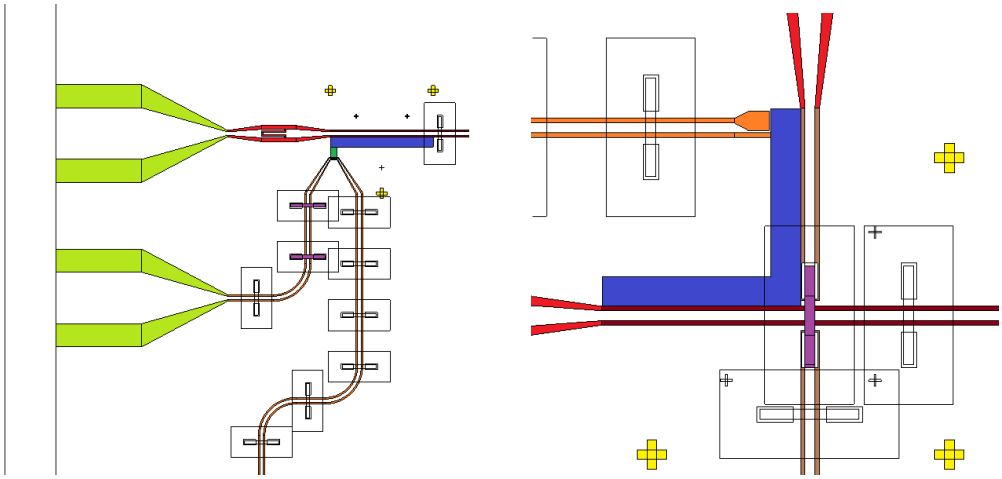

(a) A cut-out of the left side, just below the middle of Fig. 12.

(b) A cut-out of the left side, in the top, of Fig. 12.

Figure 13: An augmentation of the structures on the chip. The different elements are colored, color available online.

visible in Fig. 13a) are needed to adjust the capacitance. For further information about the coupling, see [19].

- The blue structure is the place for the qubit. It can't be fabricated in the same way as the rest of the structures (they are fabricated with photolitography) because the structures of the qubit are too small, but with e-beam lithography. Therefore some space is spared out such that in a later step of the fabrication process the exact shape of the qubit can be imprinted.

- The yellow crosses help to find the exact placement of the qubit. This is important, like this the e-beam lithography can be well adjusted.

- The green box in Fig. 13a is just a gap to separate the qubit from the flux line. This reduces the magnetic flux through the qubit. In most experiments this box wont be used.

- The orange, lengthy structures are the flux lines. They are connected to at least one pin, allowing to send a current through them. In Fig. 13a the flux line (the curvy line) is again lead to a pin, which is the better better way to do it (in this case, no unwanted currents flow on the ground). But if there are too few pins, one can just shorten the flux line to ground, as it is done in Fig. 13b. There, the flux line comes from a pin, goes along the qubit, and is shorted to ground (there is still a

little conducting band between qubit and the bulky part of the end of the flux line connecting the flux line to ground).

- The violet structures are air bridges. They are really three dimensional structures on the chip (which is absent of these entirely two dimensional). They are used to connect the two sides of a wave guide. This is done to avoid unwanted modes and to equilibrate potential of the ground. In Fig. 13b it is used to get the connection of one resonator above the other. The boxes around the bridges (not colored) are needed for the fabrication process.

- The dark red CPWs (as well as the brown CPW in Fig. 13b) are coplanar waveguide resonators. They are used to couple two qubits. They act as resonators because the photons in them are reflected at the coupling capacitances (the red structures) [19]. The length of the resonators determines their resonance frequency. To adjust their length, there are "wiggles" in the resonators (visible in Fig. 12).

- The squares in the corners of the chip (not visible in Fig. 13, but visible in Fig. 12) are made to have reference points for the alignment during the photo lithography process.

3.2 Teleportation of a Quantum State

One way to perform computations on qubits is given by only using teleportation and single-qubit operations, see [16]. Performing a quantum teleportation (compare section 2.9) on a chip is a relatively new experiment. For this reasion, it has to be tested further on.

Here, we will put two identical (mirror-symmetric) experiments on one chip, such that one can make two experiments with the effort of making only one. This again means, that we have less pins to control the qubits. Therefore, we will just use flux lines to alter the magnetic flux through the qubit and thus changing its transition frequency, compare section 2.5. These flux lines have the advantage that they do not necessarily need two pins for the current to run, but the current can just flow to the ground of the chip.

For this experiment, two different designs were realized. The first design is shown in Fig. 14, the second was already shown in Fig. 12. There is something a bit special in this experiment: we have L-shaped qubits. This is because we want to couple both resonators well with this qubit, but the coupling of the resonators between each other should be as small as possible. Therefore, the distances between the resonators are generally tried to be held as large as possible. And as well the distances between flux lines and resonators (and

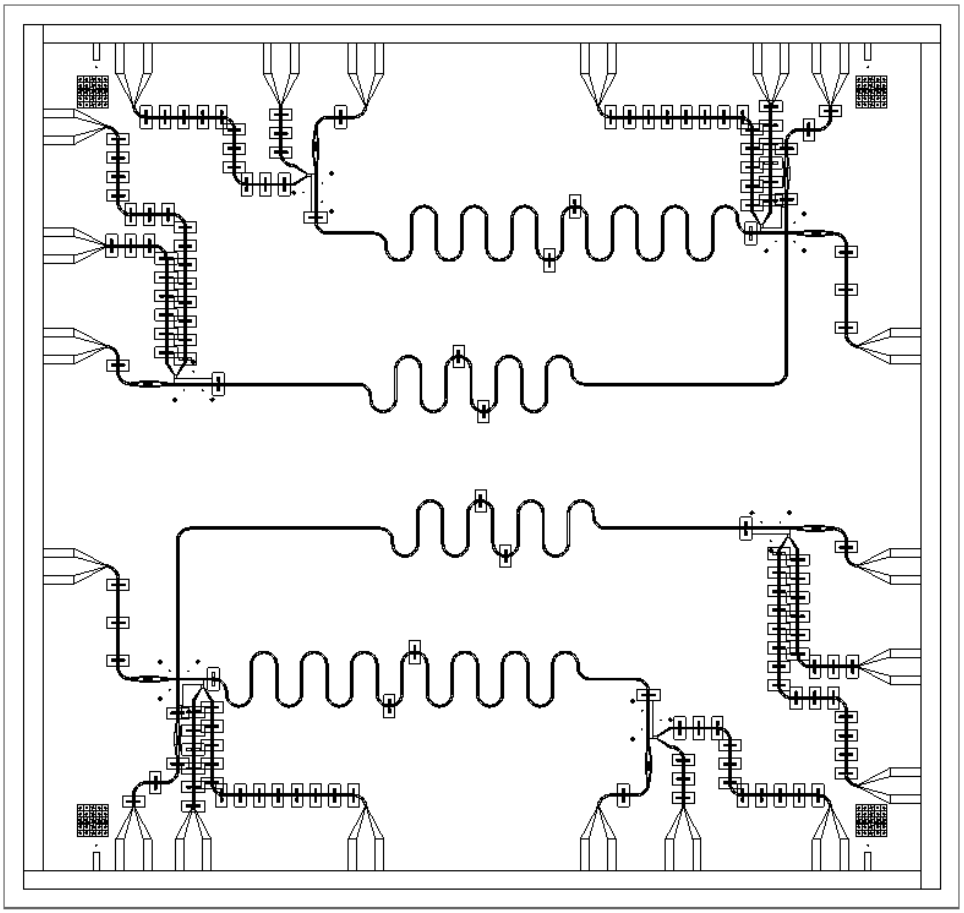

Figure 14: An alternative chip design of a quantum teleportation experiment. There are two identical experiments on the same chip, such that the effort of measuring one experiment is smaller.

between two flux lines) are tried to be maximized. This is because coupling could occur, resulting in unwanted modes in resonators. This of course would disturb the experiment.

Out of these reasons, in the first design, compare Fig. 14, the flux lines are relatively far away from the resonators. This is not really true for the upper right corner, but for the left half it is nicely done. One possible drawback of this design is that all the resonators are essentially parallel. This means, that we potentially have a high coupling. There is a possibly problematic spot in the upper right corner: the flux line is not guided back to a pin, but is just shorted to ground. This could result in a noisy ground, possibly influencing the resonator. But it is hoped that this won't influence the resonator too much, since there is a bridge over the resonator allowing the current to flow in

the area to the right. Also, there is no air bridge connecting the more central (e.g. in the upper experiment the lower) resonator to the upper coupler and the pin.This makes that resonator hardly couples with the qubit, because the wave in the resonator will be reflected at the end with the missing bridge. Therefore the resonator is not near enough to the qubit for the wave to couple. Thus, the experiment is not expected to work. But this is not very bad, since a second and more promising approach for this experiment was designed.

In the second design (Fig. 12), the resonators of one experiment are orthogonal to each other. This reduces the coupling between them. The vertical resonator is connected with an air bridge to its upper part. The flux line there is again directly shorted to ground, but the current can flow away over the many air bridges there. In the upper right corner, we have a flux line going parallel to the feed line of the coupler for a relatively large distance. This will not lead to bad results, because these two lines belong to different experiments.

Note, that to reduce the effort, only one of the two experiments was really designed. The rest was done by adding a rotated copy of the first experiment to what was already designed. The rotation is performed around the axis perpendicular to the plane of the chip in the middle of the chip.

3.3 Coupling of Resonators

Another interesting question is, how much the resonators couple to each other. And whether it is possible, to realize a design related to the one proposed in [20]. The idea there is to place the qubits like on a chess board. They are connected with resonators which form a grid. This has the advantage, that two qubits could communicate with each other only one intermediate qubit. Of course, this is not a realistic design in near future, since it requires a multilayer-chip. And this is with the fabrication methods of nowadays not possible. None the less it is useful to know whether it could work out or not.

As shown in Fig. 15, 8 resonators are crossed in the middle. It is tried to maximize the space between the resonators before they come together in the middle, such that we can investigate the coupling at a crossing. This is not so easy, since the resonator need to have a certain length. Therefore, some of the resonators are placed diagonal. This allows a better usage of the available space, and the resonators being less parallel, thus reducing the coupling away from the middle.

The big crossing in the middle, magnified in Fig. 17, is done with the help of air bridges. The resonators are that near together (in order to maximize the coupling) that the air bridges might overlap. This means, that we do

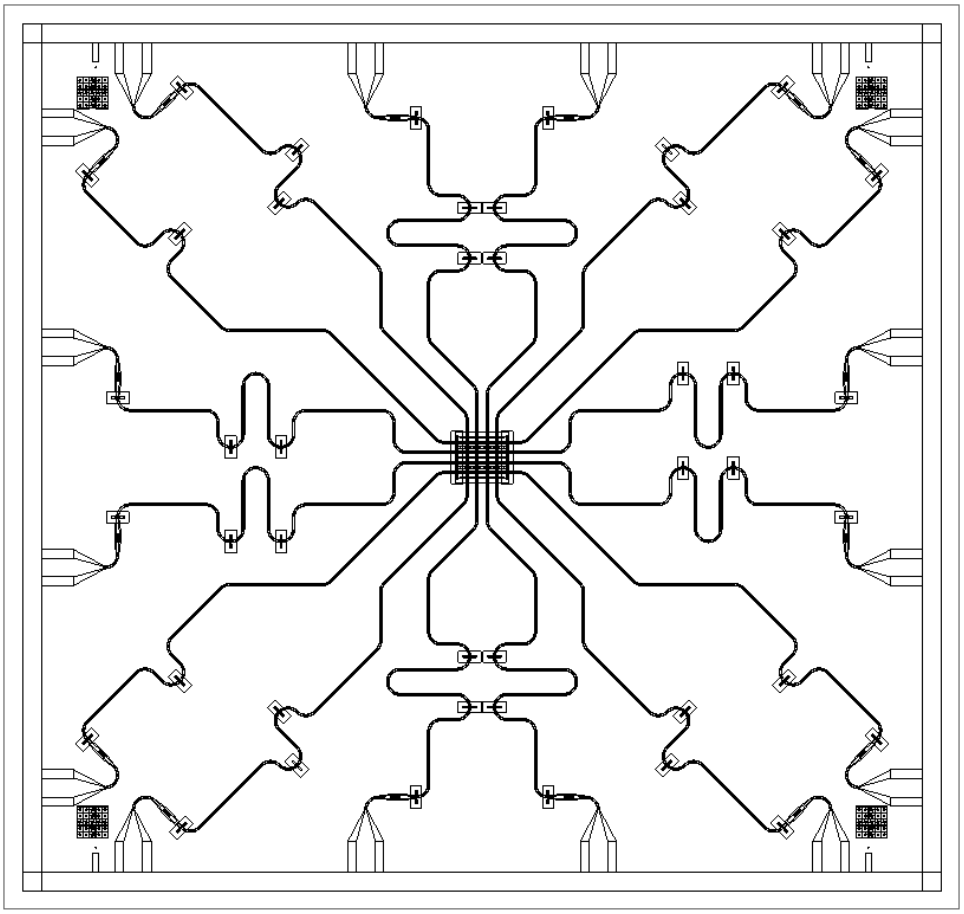

Figure 15: The chip designed to test the coupling between resonators. The 8 resonators are crossed in the middle using air bridges.

not have something like a series of bridges, but one large bridge with pillars. Between the resonators, we have as well bridges, such that the ground in the center can be equilibrated. These bridges are placed in each row and each column, between the resonators. Although some more air bridges further outside could be helpful, they are not implemented. This is because bridges are relatively delicate to fabricate, and the less of them we have the lower is the probability of fabrication mistakes.

3.4 Testing Device for Quantum Bits

A further chip is designed in order to be able to easily test different types of qubits. The more qubits that can be tested on one chip, the less is the effort per qubit. Again, we make the design mirror-symmetrical such that one can

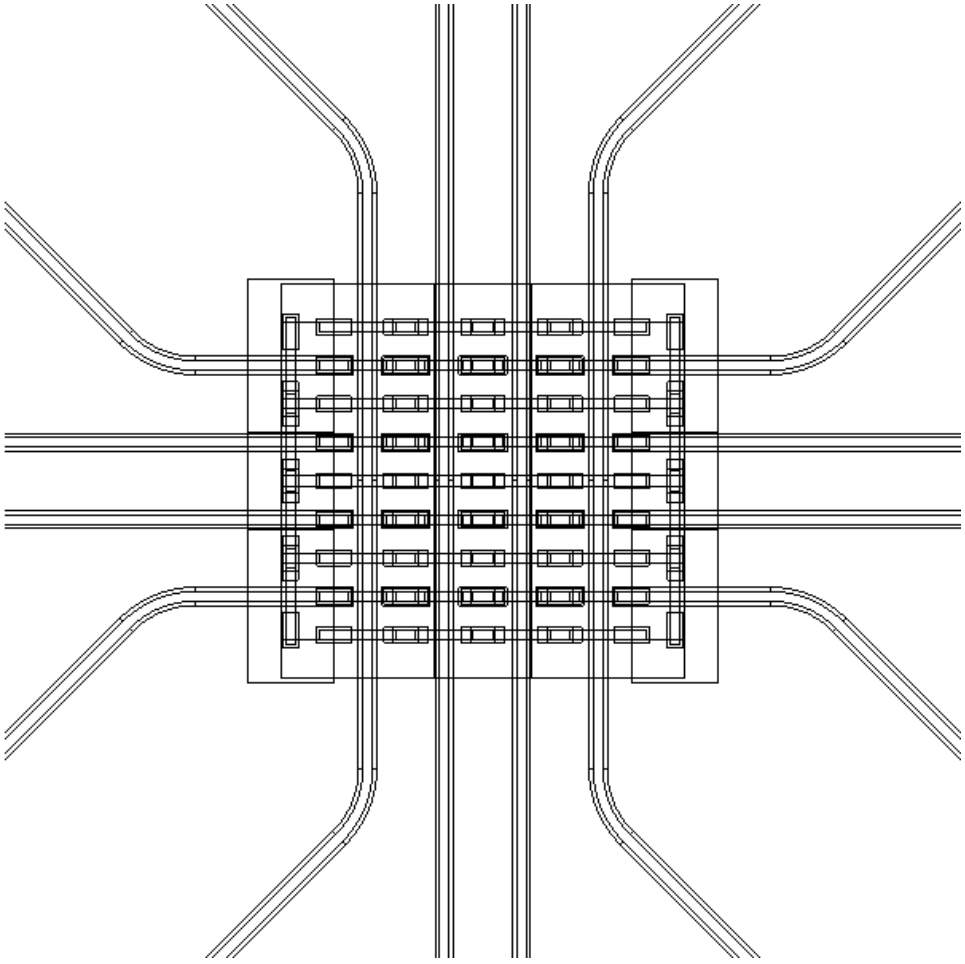

Figure 16: Magnification of the center of Fig. 15. The connecting of the resonators is done again with air bridges.

easily make two experiments. The chip is designed such that the length of the resonators can be changed by just changing a variable. This makes the design much more flexible.

The idea of this implementation is to test one qubit per time. For that, we have one big feed line, lying horizontally. It is not ended with capacitances, allowing to directly send the desired frequency through the line - of course this reduces the quality of the wave, and we have a much higher noise. The four resonators connecting the feed line with the qubits have each a different length. Thus, they all have a different resonance frequency and can be controlled independently. Because if we send the resonance frequency of say the first resonator through the feed line, only in this resonator will be a standing wave which then couples to the first qubit. In order to test the control of the

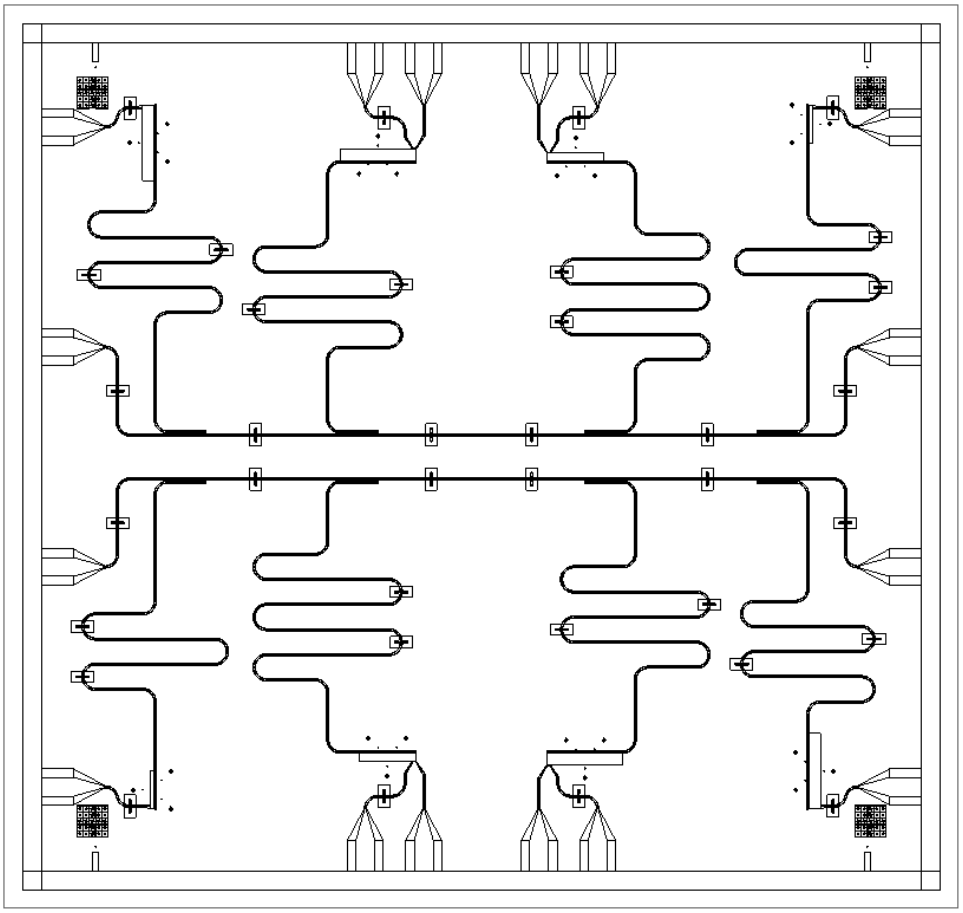

Figure 17: The chip designed to be able to easily test many qubits at the same time.

qubits, flux lines enable us to control the magnetic flux through the qubit.

Note also that the places spared out for the qubits are of different size. This is because different types of qubits shall be tested. The simulation of these is done in section 4.

3.5 A Mechanical Resonator near the Quantum Ground State

Here, an estimation is made, whether or not it would be possible to make a mechanical resonator which could be brought into it's ground state of motion. This has been implemented for example in [18]. But after a quick estimation, one has to see that this won't be that easy with the available technology: making an air bridge with an adjusted size (one pillar of the air bridges is not

build, so they form a structure like a spring board). In the following, we will make estimations for the resonator. First, we will look at the capacitance between the resonator and ground. We need a capacitance which is high enough to couple reasonably well to a coplanar wave guide resonator in order to freeze out the modes of the mechanical resonator. After that, we will look at the frequency of the mechanical resonator. It should be in the Giga-Hertz regime, such that it is in the range of the available apparatus.

We will now look at two different realizations of a quantum mechanical harmonic resonator. First, we look at a membrane like realization [17]. By integrating the resonator in an electric circuit, it is possible to cool out it's excitations. In [17] there is a technique used called sideband cooling. There, a resonator is used, which alters a capacitance by motion. Using this, it can be brought very near the ground state.

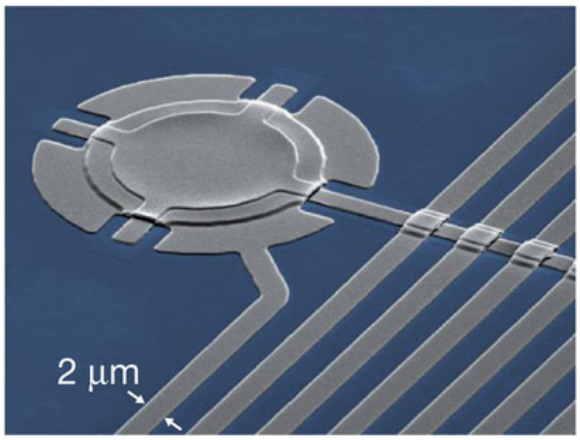

Figure 18: A 15-μm-diameter membrane in suspended 50 nm above a lower layer. The capacitance is modulated by the motion of the membrane. Figure from [17].

The idea is that a membrane (shown in Fig. 18) is suspended 50 nm above a (super-) conducting layer. The motion of the membrane then influences the capacitance between the membrane and the underlying layer. The membrane would play the role of the quantum mechanical resonator. We now want to estimate the capacitance between the layer and the the membrane. Like this, we can get an idea about how big the capacitance would have to be, and how big our resonator has to be in order to get it near the ground state. Since the membrane has a diameter of 15 μm and the distance between it an the layer below is only 50 nm, we can expect that the formula of the plate capacitor should yield appropriate results. The formula for the capacitance of a plate

capacitor is

$$C = \epsilon_0 \epsilon_R \cdot \frac{A}{d}, \tag{11}$$

where A is the surface of the capacitor and d is the distance between the plates. Since in [17] a round membrane is used, we have with $A = r^2\pi$ and because we are in the vacuum (giving us $\epsilon_R \approx 1$) that

$$C = \epsilon_0 \epsilon_R \cdot \frac{r^2\pi}{d} \approx 8.85 \cdot 10^{-12} \frac{(7.5 \cdot 10^{-6})^2 \pi}{5 \cdot 10^{-8}} \approx 3.1 \cdot 10^{-14} \text{ F} = 31 \text{ fF}. \tag{12}$$

Now we can estimate how big the surface has to be using the air bridges. They have a length $l = 40$ μm and are $d = 2$ μm above ground. Again we set ϵ_R to 1, and we get with Eq. (11) that

$$A = \frac{C \cdot d}{\epsilon_0 \epsilon_R} \approx \frac{3.1 \cdot 10^{-14} \cdot 2 \cdot 10^{-6}}{8.85 \cdot 10^{-12}} \approx 7 \cdot 10^{-9} \text{ m}^2. \tag{13}$$

This would mean that our plate capacitor has to have a width b of ($A = l \cdot b$, with $l = 40$ μm being the length of an air bridge)

$$b = A/l \approx \frac{7 \cdot 10^{-9}}{4 \cdot 10^{-5}} \approx 1.8 \cdot 10^{-4} \approx 180 \ \mu\text{m}. \tag{14}$$

This is not realistic to achieve, since an air bridge is about 10 μm wide. This would mean that we need to place 18 air bridges at least next to each other to get the same capacitance. Note that the assumption made in Eq. 14 is optimistic: we wont have that the whole 40 μm of the air bridge contribute to the capacitance like calculated as a plate capacitor. If we use as the underlying part a normal CPW (which is only 20 μm wide), only approximately half of the air bridge length will contribute to the capacitance as computed, the rest will contribute much less. Thus, we can speak of these 18 air bridges being a lower limit for the required capacity.

An other problem appears if we consider the weight of the structure. In [17] the mass of the membrane is stated as 48 pg. If we estimate the weight m of our oscillator, we get with $\rho_{Al} = 2.7 \cdot 10^6$ g/m^3 and the height $h = 800\,$nm of an air bridge that

$$m = V \cdot \rho_{Al} = hA \cdot \rho_{Al} \approx 8 \cdot 10^{-7} \cdot 7 \cdot 10^{-9} \cdot 2.7 \cdot 10^6 \approx 15 \text{ ng}. \tag{15}$$

This means, that the structure created here would be about 300 times heavier than the structure used in [17]. This again means that more energy would be needed to be frozen out, which again means more difficulties.

In another paper [18] they use a $30\,\mu$m broad, 170 nm long and 140 nm thick nanomechanical resonator which is coupled to a superconducting microwave resonator (distance to this is 75 nm), compare Fig. 19. If we roughly

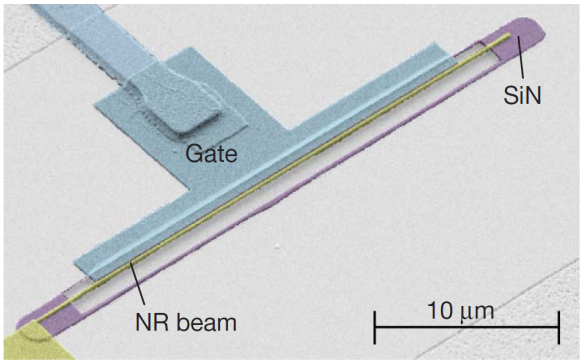

Figure 19: A nanomechanical resonator which is coupled to a superconducting microwave resonator. Figure from [18].

estimate the capacitance between ground (the superconducting microwave resonator) and the nanomechanical resonator in this case, using again the formula (11) for a plate capacitor, we get a capacitance of

$$C \approx 8.85 \cdot 10^{-12} \cdot \frac{3 \cdot 10^{-5} \cdot 1.7 \cdot 10^{-7}}{7.5 \cdot 10^{-8}} \approx 6.0 \cdot 10^{-16} \text{ F} = 0.6 \text{ fF}, \tag{16}$$

where we set $\epsilon_R = 1$. Now we compare with our resonator consisting of air bridges. We want to have the same capacitance, again in the approximation of a plate capacitor. An air bridge is $l = 40$ μm long (we take this value because we have it everywhere else, but it could be varied). With $A = l \cdot b$ we can again determine the width b of the structure with

$$b = \frac{C \cdot d}{l \cdot \epsilon_0 \epsilon_R}. \tag{17}$$

Again, we set $\epsilon_R = 1$, and use that in our case we have that $d = 2$ μm and get

$$b = \frac{6.0 \cdot 10^{-16} \cdot 2 \cdot 10^{-6}}{4 \cdot 10^{-5} \cdot 8.85 \cdot 10^{-12}} = 3.4 \text{ } \mu\text{m}. \tag{18}$$

This means, that already one air bridge would be enough and that it would be possible. But here we again assumed that the whole 40 μm of the air bridge contribute equally to the capacitance relative to the resonator. Since the width of the resonator is only about half of this, this is a strong overestimation. Also it has to be considered that our structures are more than 5 times thicker than the structures in [18]. This again leads to more difficulties in freezing out the excited states.

Compared to the membrane in [17], the values in [18] are much nearer to the ones that can be achieved here. Perhaps it would be possible to construct

a nanomechanical resonator with altered values for the air bridge: a much smaller d would be required and a much thinner bridge would also be helpful. Of course, diminishing the d will lead to difficulties in the fabrication process.

But the capacitance of the air bridge to the wave guide is not the only thing we have to consider. It is also very important, that resonance frequency of the structure is in the frequency range we can handle. This is about 2-8 GHz, thus the same frequency range where all the resonance frequencies of the resonators on the chips are (and the apparatus available runs). Therefore the resonance frequency ω_0 of the resonator has to be estimated. Since our resonator is essentially a microscopic cantilever, we will use Stoney's formula (or also see [21]) to compute the resonance frequency ω_0 of the resonator

$$\omega_0 = \sqrt{\frac{Ewt^3}{4l^3 m_{eq}}}, \tag{19}$$

where E is Young's modulus, L the length of the air bridge, t its thickness,w its width and m_{eq} its equivalent mass. We will approximate the equivalent mass with the mass of the air bridge, and thus we can write

$$\omega_0 = \sqrt{\frac{Ewt^3}{4l^3 wtl\rho}} = \sqrt{\frac{Et^2}{4l^4\rho}}, \tag{20}$$

where ρ is the density of the material. It is now clear, that the resonance frequency does not depend on the width of the resonator. If we use the values we took to estimate the capacitance, $t = 800\,\text{nm}$ and $l = 40\,\mu\text{m}$ and use that Young's modulus for Al is $E = 69\,\text{GPa}$ and the density of Al is $\rho = 2700\,\text{kg/m}^3$, we get that

$$\omega_0 = \sqrt{\frac{Et^2}{4l^4\rho}} = \sqrt{\frac{69\cdot 10^9\cdot(8\cdot 10^{-7})^2}{4\cdot(4\cdot 10^{-5})^4\cdot 2.7\cdot 10^3}} = 1.3\cdot 10^6 \quad 2\pi/\text{s}. \tag{21}$$

This value is much too low, being only in the MHz regime whereas it should be in the order of GHz. In order to get to higher frequencies we can either take other materials (which wont get us a factor of 10^3) or increase the thickness or decrease the length of the resonator. Since increasing the thickness will make ω_0 only to increase linearly, this is not very interesting. Reducing the length will make ω_0 to increase in quadratic order. If we want to increase ω_0 by a factor of 10^3, we have to reduce l by a factor of $\sqrt{1000} \approx 31.6$ resulting in a length $l \approx 1.3\,\mu\text{m}$. Such a tiny length of course will diminish the capacitance between resonator and the wave guide to a very low value. And with such a low capacitance it wont be possible to cool the resonator down into the ground state any more.

It has to be noted that in [17] a technique called sideband-cooling is used. This technique makes it possible to control an oscillator in the MHz regime with a GHz apparatus. This means, that a mechanical resonator like this one here could be brought into its ground state of motion, using sideband-cooling and a GHz apparatus.

4 Transmon Simulations

To fabricate and measure each design of a Transmon is a big effort. It is much easier to simulate them on a computer. Analyzing the important quantities enables to exclude designs with unwanted properties. This reduces the amount of Transmons to be produced and measured, thus saving costs and work.

Simulating some Transmons and trying to improve their properties was a task of this thesis too. To do so, the program Maxwell 14.0 by ANSYS has been used. The qubit and it's near surrounding on the chip has been extracted from Mathematica and imported into Maxwell. There, the the sapphire substrate (this is where all the elements are placed on) has additionally been created, compare Fig. 20. After that, excitations could be assigned to the different elements, and Maxwell calculated the capacities of the pieces to each other. This is done with the method of finite elements. With these values, all the important quantities can be calculated.

4.1 Important Quantities

Maxwell calculates the capacities between the different areas of the model. These are the resonator, the ground, the reservoir, the island and the flux line. Out of these, the three quantities can be calculated:

- The charging energy $E_C = e^2/2C_\Sigma$, where C_Σ is the capacitance between island and reservoir (compare section 2.4). We will in the following try to minimize E_C, given certain constrictions.
- The coupling g_{res} between the resonator and the island. This quantity is not as critical as E_C: it is normally large enough, and if it should be lowered, one can simply move the qubit away from the resonator.
- The coupling g_{flux} between the reservoir and the flux line. This quantity is not as important as E_C either.

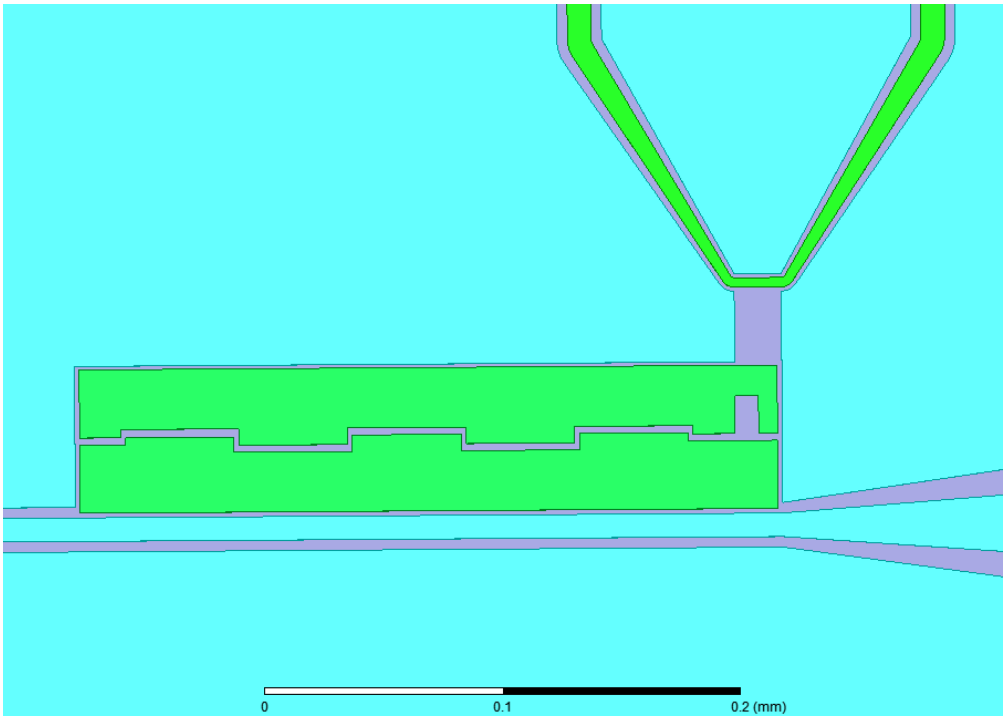

Figure 20: A picture of a simulated Transmon. The upper green part is a fluxline, and the central parts are the island (near the resonator) and the reservoir (near the flux line). Below them there is a resonator and at the right side we have the coupler. The light blue area is the aluminum ground of the chip (this is a thin superconducting aluminum layer). The gray area is the sapphire substrate on which everything is placed.

Additionally, the design should - as good as possible - minimize the electric field between the components. This is because strong electric fields are suspected to have a negative effect on the coherence time.

Bringing two structures closer together enlarges the capacitance between them. Thus, if we want a strong coupling between the resonator and island (a large g_{res}) we can move the resonator nearer to the island.

4.2 Minimizing E_C

If the reservoir and the island are separated only by a small distance, the capacitance between them will be high. This again means, that E_C is lowered. But this is not the best thing one can do, because if two structures are moved together, the electric field in between becomes stronger. Note that the approximation of plate capacitors can not be used here, since the distance

between the structures is big compared to the extension of the surfaces facing each other (the structures are only 200 nm thick). This means, that one has to find a compromise between high capacitance and low electric field.

Trying to lower E_C means to increase the capacitance between reservoir and island. The most promising way to increase the capacitance between reservoir and island is to increase their dimensions. This means, instead of making the qubit with measures 300 times 60 μm, one can make them twice as long to 600 times 60 μm (a qubit with such dimensions is shown in Fig. 21) and with that double the capacitance between island and reservoir. The maximal magnitude of the electric field is not affected by this enlarging, since the relevant parameters for it remain untouched.

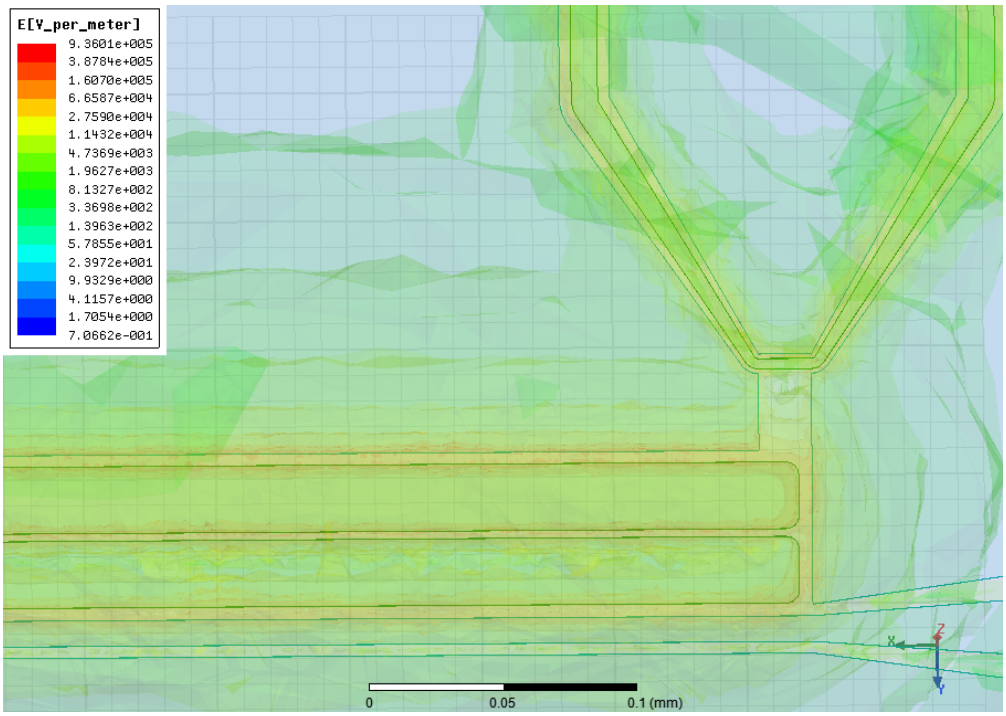

Figure 21: A picture of a simulated qubit with a length of 600 μm. The gap between island and reservoir is 3 μm and the distance to ground is 5 μm everywhere. The scale of the electric field is logarithmic.

Another method to increase the capacitance is to make a structure with fingers. For example, the qubit shown in Fig. 20 has such fingers. The disadvantage of these fingers is that they have many corners. And at corners, we have a strong electric field (compare next section).

4.3 Minimizing the Electric Field

As mentioned above, the simplest way to reduce the electric field between components is to separate them by big distances. But this not only brings down the electric field, but also the capacitance between the components. This is not desired, since E_C should be minimized.

Another idea to reduce the electric field is to avoid sharp edges in the corners and make round corners instead. This is because at a sharp apex the electric field is very strong (at a perfect apex we would have a diverging electric field), compare for that [22, Chapter 3.4]. To look at this more precise, a special simulation was done, compare Fig. 22. In this simulation,

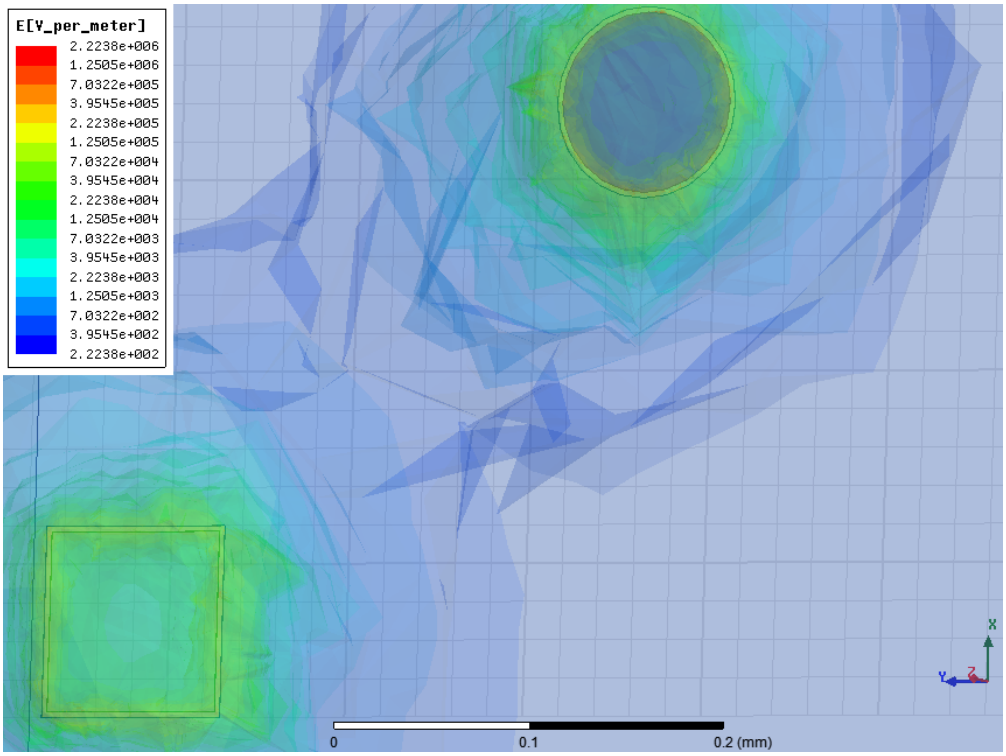

Figure 22: A picture of the simulated setup to determine the electric field of circular and rectangular geometries. The scale of the electric field is logarithmic.

the dimensions and the materials assigned to the structures are the same as in the simulation of the qubits. The electric field is displayed with a logarithmic magnitude plot. No big difference can be seen between the field strengths of the circle and the square. This is due to the fact that the circle consist of a polygon with some 24 edges. This is not smooth enough to make the

difference really visible. Furthermore, if one zooms in to the edges of the polygon, one can see that the electric field magnitude is dominated by these. So, it is not really clear whether this method can bring a big advantage. The qubit therefore has probably to be fabricated and tested for finding it out.

4.4 Results

The most important results found by simulating different qubits are listed below.

- It seems that the best way to both minimize the electric field and E_C is to choose larger dimensions for the qubit.
- The round edges do not lower the magnitude of the electric field in the simulations.
- The size of the gap between reservoir and island has the much lower effect on the capacitance between them than the length of the qubit.
- Also, the effect of making fingers is rather small compared to choosing larger dimensions.
- Both, g_{res} and g_{flux} can be controlled easily by altering the distance between the qubit and the resonator, respectively the flux line.
- Separating island and reservoir by a relatively big distance (at least 5 μm) from ground decreases the electric field without altering E_C.

5 Conclusion

The designs of three different experiments with superconducting quantum bits were made. The first design was realized to perform a quantum teleportation. The second experiment aims to understand the coupling between resonators more exact. And the third design is made to be able to study the properties of different quantum bits.

After this, several different designs for qubits were simulated. The numbers for E_C and the magnitude plots of the electric field indicate, that a long qubit (600 times 60 μm) should yields good results. Also, the qubit should be without fingers and there should be a distance of 5 μm separating ground, island and reservoir. The distance between the components lowers the amplitude of the electric field, and the larger dimension of the qubit improves the capacitance between island and resonator. The influence of round

corners could not be evaluated by simulation, but should be tested on really fabricated qubits.

Neither the designed experiments nor the qubits were tested and measured yet. This of course makes it not possible to say whether the designs were good or not.

6 Outlook

Of course, the designed experiments now need to be fabricated. After that, one can measure the properties of the chips, and look whether the experiments work or not.

For the simulations of the qubits, a more systematic approach is needed. With that, it will be possible to understand better the dependences of the interesting quantities on the parameters. At the moment, another semester thesis is being done about exactly this subject.

7 Acknowledgment

I would like to thank Prof. A. Wallraff for making this semester project possible. It was a great experience for me to make such an interesting project. I also would like to thank my supervisor Lars Steffen for his valuable guidance and the rest of the group for the nice atmosphere.

References

[1] Lloyd, S. The computational universe: Quantum gravity from quantum computation. quant-ph/ 0501135 (2005).

[2] Fink, J. Master thesis, Universität Wien, 2007.

[3] Devoret, M. H., Wallraff, A., and Martinis, J. M. Superconducting qubits: A short review. cond-mat/ 0411174 (2004).

[4] Shor, P. W. Polynomial-time algorithms for prime factorization and discrete logarithms on a quantum computer. Siam J. Sci. Statist. Comput. 26, 1484 (1997).

[5] Grover, L. K. A fast quantum mechanical algorithm for database search. In STOC 1996: Proceedings of the twenty-eighth annual ACM symposium on Theory of computing, 212-219 (ACM Press, New York, NY, USA, 1996).

[6] Wallraff, A., Schuster, D. I., Blais, A., Frunzio, L., Huang, R. S., Majer, J., Kumar, S., Girvin, S. M., and Schoelkopf, R. J. Strong coupling of a single photon to a superconducting qubit using circuit quantum electrodynamics. Nature 431(7005), 162-167 (2004).

[7] Steffen, L. Master thesis, ETH Zürich, 2008.

[8] L. Frunzio, A. Wallraff, D. Schuster, J. Majer, and R. Schoelkopf. Fabrication and characterization of superconducting circuit QED devices for quantum computation. IEEE Transactions On Applied Superconductivity, 15(2):860-863, June 2005.

[9] D. I. Schuster. Circuit Quantum Electrodynamics. PhD thesis, Yale University, 2007.

[10] Bouchiat, V., Vion, D., Joyez, P., Esteve, D., and Devoret, M. H. Quantum coherence with a single Cooper pair. Physica Scripta T76, 165-170 (1998).

[11] Koch, J., Yu, T. M., Gambetta, J., Houck, A. A., Schuster, D. I., Majer, J., Blais, A., Devoret, M. H., Girvin, S. M., and Schoelkopf, R. J. Introducing the transmon: a new superconducting qubit from optimizing the cooper pair box. cond-mat/ 0703002v1 (2007).

[12] Jens Koch, Terri M. Yu, Jay Gambetta, A. A. Houck, D. I. Schuster, J. Majer, Alexandre Blais, M. H. Devoret, S. M. Girvin, and R. J. Schoelkopf. Chargeinsensitive qubit design derived from the Cooper pair box. Physical Review A, 76(4):042319, 2007.

[13] A. Blais, R. S. Huang, A. Wallraff, S. M. Girvin, and R. J. Schoelkopf. Cavity quantum electrodynamics for superconducting electrical circuits: An architecture for quantum computation. Physical Review A, 69(6):062320, June 2004.

[14] W.K. Wootters and W.H. Zurek, A Single Quantum Cannot be Cloned, Nature 299 (1982), pp. 802-803.

[15] D. Bouwmeester, J.-W. Pan, K. Mattle, M. Eibl, H. Weinfurter, A. Zeilinger. Experimental Quantum Teleportation, Nature 390, 6660, 575-579 (1997).

[16] Daniel Gottesman & Isaac L. Chuang. Demonstrating the viability of universal quantum computation using teleportation and single-qubit operations, Nature 402 , 390-393 (1999).

[17] J. D. Teufel, T. Donner, Dale Li, J. W. Harlow, M. S. Allman, K. Cicak, A. J. Sirois, J. D. Whittaker, K. W. Lehnert & R. W. Simmonds. Sideband cooling of micromechanical motion to the quantum ground state, Nature 475, 359-363 (2011).

[18] T. Rocheleau, T. Ndukum, C. Macklin, J. B. Hertzberg, A. A. Clerk & K. C. Schwab. Preparation and detection of a mechanical resonator near the ground state of motion, Nature 463, 72-75 (2010).

[19] M. Göppl, A. Fragner, M. Baur, R. Bianchetti, S. Filipp, J. M. Fink, P. J. Leek, G. Puebla, L. Steffen, and A. Wallraff. Coplanar Waveguide Resonators for Circuit Quantum Electrodynamics, J. Appl. Phys. 104, 113904 (2008).

[20] F. Helmer, M. Mariantoni, A. G. Fowler, J. von Delft, E. Solano and F. Marquardt. Cavity grid for scalable quantum computation with superconducting circuits, EPL 85 50007 (2009).

[21] Clark T.-C. Nguyen and Roger T. Howe. An Integrated CMOS Micromechanical Resonator High-Q Oscillator, IEEE J. of Solid-State Circuits, Vol. 34, No. 4 (April 1999).

[22] J. D. Jackson, Klassische Elektrodynamik, 4. Auflage (de Gruyter, 2006).